Photochemical Synthesis and Stereophysical Characterization of $W(CO)_4[cyclo\text{-}(PW(CO)_5)_4]$: Experimental–Theoretical Bonding Analysis of Its Unprecedented Pentametal-Coordinated *cyclo*-P_4 Ligand

Mary E. Barr,[1a,b] Scott K. Smith,[1a] Brock Spencer,[1c] and Lawrence F. Dahl*,[1a]

Departments of Chemistry, University of Wisconsin—Madison, Madison, Wisconsin 53706, and Beloit College, Beloit, Wisconsin 53511

Received March 5, 1991

A photochemical reaction of elemental white phosphorus (P_4) with $W(CO)_6$ has resulted in the isolation (in 67% yield) of $W(CO)_4[cyclo\text{-}(PW(CO)_5)_4]$ (1), which is only the second example of a metal complex containing a *cyclo*-P_4 ligand. 1 was characterized by single-crystal X-ray diffraction, laser-desorption FT mass spectrometric, solution ^{31}P, ^{13}C, and ^1H NMR, solid-state ^{31}P NMR, infrared, and electrochemical measurements. This complex possesses a novel pentametal-coordinated *cyclo*-P_4 ligand, which is linked not only to an apical $W(CO)_4$ fragment by its four π electrons but also to four Lewis-acid $W(CO)_5$ fragments by its four normally unshared electron pairs. Evidence that the *cyclo*-P_4 ligand possesses an instantaneous C_s-*m* kite-shaped geometry (which was not detected in the X-ray diffraction study due to the molecule possessing crystallographic C_4-4 site symmetry) is given by solution ^{31}P NMR spectra, which exhibit three resonances with an AM_2X pattern at room temperature in high-polarity solvents and at lower temperatures in low-polarity solvents. Of particular interest is that a recent X-ray crystallographic determination of $Nb(\eta^5\text{-}C_5Me_5)(CO)_2P_4$ (2) revealed that its *cyclo*-P_4 ring is slightly distorted from a square configuration toward a planar C_s-*m* kite-shaped configuration in accordance with molecular pseudo-C_s symmetry. A low-temperature solution ^{31}P NMR spectrum of 2 also exhibited three well-resolved signals, which were attributed to hindered rotation of the *cyclo*-P_4 ligand. That a presumably analogous C_s-*m* kite-shaped configuration is exhibited by the *cyclo*-P_4 ligand in both 1 and 2, which have cylindrical C_4 and noncylindrical C_s symmetry, respectively, provides convincing evidence that this distortion of the *cyclo*-P_4 ligand in solution is due solely to electronic interactions involving the π-coordinated metal–ligand fragment and appears to be independent of the overall molecular symmetry. Unfortunately, room- and low-temperature solid-state ^{31}P NMR spectra of 1 did not yield additional information about the *cyclo*-P_4 ring. Molecular orbital calculations were carried out with the nonparametrized Fenske–Hall model on the hypothetical $W(CO)_4P_4$ molecule and on 1 in order to describe the bonding of a *cyclo*-P_4 unit π-coordinated to a metal tetracarbonyl fragment of overall C_4 symmetry. The MO results revealed that the doubly degenerate HOMOs in $W(CO)_4(\eta^4\text{-}P_4)$ are primarily composed of slightly antibonding in-plane *cyclo*-P_4 orbitals, while the doubly degenerate LUMOs mainly possess bonding $W(5d_\pi)$–$CO(\pi^*)$ orbital character with smaller contributions of antibonding $W(5d_\pi)$–$P(3p_\pi)$ orbital character. The main contributors to the doubly degenerate HOMOs of 1 are nonbonding $W(CO)_5$ orbitals; the much higher energy LUMOs remain essentially unchanged in orbital character. Hence, the MO calculations are consistent with the observed irreversible electrochemical behavior of 1 but provide no clear-cut explanation for a distortion of the *cyclo*-P_4 ligand. 1 crystallizes as solvated $1\cdot CH_2Cl_2$ in two nonseparated crystalline forms. X-ray crystallographic studies showed that both forms have tetragonal unit cells of virtually identical volumes (with $Z = 2$) but of different symmetries (*P4nc* versus *I4*); structural analyses showed that 1 has an analogous molecular configuration in both crystal forms. The formulation of 1 as $W_5(CO)_{24}P_4$ was confirmed from a positive-ion LD/FT mass spectrum, which showed the existence of the parent-ion peak envelope ($m/z \sim 1714$).

Introduction

Although transition-metal complexes containing 3π *cyclo*-P_3 units have been studied for a number of years, syntheses and structural determinations of compounds containing larger $n\pi$ *cyclo*-P_n ($n = 5, 6$) units are a more recent development. Reviews[2,3] of these metal-coordinated *cyclo*-P_n ($n = 3, 5, 6$) complexes, as well as studies of the electronic structures[4] of these and related inorganic ring "sandwich" complexes, provide an excellent perspective of the development of this area of transition-metal phosphido chemistry.

In contrast to the relatively large number of transition-metal complexes containing π-bonded P_3, P_5, and P_6 rings, systems with a *cyclo*-P_4 unit are rare. In fact, the compound presented herein, $W(CO)_4[cyclo\text{-}(PW(CO)_5)_4]$ (1), is only the second reported complex with a fully bonding *cyclo*-P_4 ligand, and it is the only metal carbonyl complex containing a *cyclo*-P_n ring where $n > 3$ that does not also contain $\eta^5\text{-}C_5R_5$ ligands. While this research was in progress, Scherer et al.[5] reported the preparation and characterization of $NbCp^*(CO)_2P_4$ (2) (where Cp* denotes $\eta^5\text{-}C_5Me_5$); this compound was synthesized via a photolytic procedure similar to that used in our laboratory to generate 1, rather than by the more commonly used thermolytic synthetic route. A crystallographic analysis of 2 revealed that the four niobium-coordinated phosphorus atoms of its *cyclo*-P_4 ring are coplanar and form a slightly distorted (kite-shaped) square that conforms to an overall pseudo-mirror-plane symmetry. Another recently reported com-

(1) (a) University of Wisconsin—Madison. (b) Present address: Los Alamos National Laboratory, University of California, Los Alamos, NM 87545. (c) Beloit College.

(2) (a) Di Vaira, M.; Stoppioni, P.; Peruzzini, M. *Polyhedron* **1987**, *6*, 351. (b) Di Vaira, M.; Sacconi, L. *Angew. Chem., Int. Ed. Engl.* **1982**, *21*, 330.

(3) (a) Scherer, O. J. *Angew. Chem., Int. Ed. Engl.* **1985**, *24*, 924. (b) Scherer, O. J. *Comments Inorg. Chem.* **1987**, *6*, 1. (c) Scherer, O. J. *Nachr. Chem. Tech. Lab.* **1987**, *35*, 1143.

(4) (a) Tremel, W.; Hoffmann, R.; Kertesz, M. *J. Am. Chem. Soc.* **1989**, *111*, 2030. (b) Jemmis, E. D.; Reddy, A. C. *Organometallics* **1988**, *7*, 1561.

(5) Scherer, O. J.; Vondung, J.; Wolmershäuser, G. *Angew. Chem., Int. Ed. Engl.* **1989**, *28*, 1355.

0276-7333/91/2310-3983$02.50/0

plex, $Rh_2(C_5Me_4Et)_2(CO)(\eta^4\text{-}P_4)$,[6] contains a dibridging 4π η^4-P_4 unit with an open-edge butadienyl-type bonding configuration instead of a *cyclo*-P_4 ring.

$W_5(CO)_{24}P_4$ (1) was synthesized during our investigation of the photolytic generation of transition-metal polyphosphido complexes from metal carbonyl or organometallic precursors and elemental white phosphorus.[7] Since 1 is the only known *cyclo*-P_4 complex in which the phosphorus ring is both σ- and π-coordinated to metal fragments, it provides unique information regarding the configuration and bonding of the P_4 ring. Reported herein are the details of the synthesis and stereophysical analysis of 1 via X-ray crystallographic, mass spectrometric, variable-temperature solution ^{31}P, ^{13}C, and ^1H NMR, solid-state ^{31}P NMR, infrared, and electrochemical studies. Molecular orbital calculations on the hypothetical $W(CO)_4P_4$ molecule and on 1 were performed with the Fenske–Hall nonparametrized model;[8] comparison of the hypothesized kite-shaped geometry of the *cyclo*-P_4 ligand with theoretical determinations of optimal configurations for the electronically equivalent cyclobutadiene ligand are discussed.

Experimental Section

General Procedures. All reactions, sample transfers, and manipulations were performed with oven-dried standard Schlenk-type glassware under nitrogen, either on a vacuum line, in a glovebag, or in a Vacuum Atmospheres glovebox. The following solvents were dried and distilled prior to use: THF (K/Ph_2CO), CH_2Cl_2 (CaH_2), $CHCl_3$ (CaH_2), CH_3CN ($CaSO_4$), and hexane (Skelly B cut, CaH_2). P_4 (Strem) and $P(C_6H_5)_3$ and $W(CO)_6$ (Pressure Chemical Co.) were used without further purification.

Solution and solid-state infrared spectra were recorded on a Beckman 4240 spectrometer. Solution multinuclear NMR spectra were obtained with Bruker AM-500 (^{31}P), Bruker AM-360 (^{13}C), and Bruker WP-270 (^1H, ^{31}P) spectrometers. Solid-state ^{31}P NMR spectra were obtained with a Varian Unity-300 spectrometer. Cyclic voltammograms were obtained with a BAS-100 electrochemical analyzer with the electrochemical cell enclosed in a nitrogen-filled Vacuum Atmospheres glovebox. Electrochemical measurements were carried out in CH_2Cl_2 and THF solutions conaining 0.1 M $[NBu_4]^+[PF_6]^-$ as the supporting electrolyte. The working electrode was a platinum disk, and the reference electrode was a Vycor-tipped aqueous SCE separated from the test solution by a Vycor-tipped salt bridge filled with a 0.1 M $[NBu_4]^+$-$[PF_6]^-/CH_3CN$ solution. The auxiliary electrode was a platinum coil. Each test solution consisted of ca. 7 mL of solvent containing approximately 10^{-3} M compound. An *iR* compensation for solution resistance[9] was made before current–voltage curves were obtained.

Mass spectra were obtained with an EXTREL FTMS-2000 Fourier transform (FT) mass spectrometer equipped with a 3.0-T superconducting magnet, an EXTREL laser-desorption (LD) interface, and a Tachisto 215G resonator. Additional details of the LD-FTMS instrument and procedures for sample preparation and data collection are available elsewhere.[10]

Table I. Crystal, Data-Collection, and Structural Refinement Parameters for $W_5(CO)_{24}P_4 \cdot CH_2Cl_2$ ($1 \cdot CH_2Cl_2$)

	P4nc	*I4*
fw	1800.3	1800.3
cryst system	tetragonal	tetragonal
cell const temp, °C	−100	−50
$a = b$ Å	12.205 (4)	12.092 (1)
c, Å	14.503 (6)	14.785 (3)
$\alpha = \beta = \gamma$, deg	90	90
V, Å^3	2160 (2)	2162 (1)
space group	*P4nc*	*I4*
Z	2	2
d_{calcd}, g/cm^3	2.77	2.77
μ, mm^{-1}	13.9	13.9
data collcn temp, °C	−100	−50
radiation	Mo Kα	Mo Kα
scan mode	Wyckoff	Wyckoff
scan speed, deg/min	2–12	2–11
scan range, deg	0.8	1.1
background offset, deg	1.0	1.0
2θ limits, deg	4–52	5–50
no. of data collcd	3246	3502
cutoff for obsd data	$\|F\| > 3\sigma(F)$	$\|F\| > 3\sigma(F)$
no. of ind obsd data	1168	798
data/param	8/1	10/1
wght	0.000 35 (ref)	0.0005 (fix)
goodness-of-fit, GOF	1.50	2.17
$R_1(F)$, $R_2(F)$, %	6.13, 5.88	6.85, 7.11

Preparation and Physical Properties of $W_5(CO)_{24}P_4$ (1). In a typical reaction, $W(CO)_6$ (1.58 g; 4.5 mmol) and P_4 (0.28 g; 2.2 mmol) in a 2:1 P atom:W atom ratio were each dissolved in ~100 mL of THF, and the solutions were transferred into a water-cooled Pyrex photolysis apparatus equipped with a 450-W Hanovia medium-pressure Hg-vapor lamp. The solution was irradiated until IR spectra exhibited no further changes in the terminal carbonyl region (~2–3 h). The solution was then concentrated to ca. 20 mL under vacuum, cooled in a dry ice/ethanol slush bath to precipitate unreacted $W(CO)_6$ and P_4, and decanted. After removal of the solvent from the decantate under vacuum, the resultant red, glassy solid was washed with hexane (2×) to remove any remaining P_4 and then extracted with CH_2Cl_2 (3×). The orange/red CH_2Cl_2 extracts were combined and reduced to 15–20 mL under vacuum, at which point an orange precipitate formed. This mixture was heated gently in a warm water bath (ca. 60 °C) to redissolve the solid and then cooled slowly over ~1 h to −78 °C in a thermally buffered dry ice/ethanol bath. Orange, crystalline 1 (1.08 g; 0.60 mmol; 67% yield) precipitated. The deep red, oily supernatant exhibited an infrared spectrum similar to that of the original solution, but further concentration/cooling cycles resulted in the precipitation of only a minimal amount of additional product.

1 is an orange crystalline solid which is moderately air-stable. The ease of crystallization and solubility of 1 vary greatly with the choice of solvents; in chlorinated solvents such as CH_2Cl_2 and $CHCl_3$, 1 exhibits notable temperature-dependent solubility and crystallizes readily, but all attempts at crystallization in nonchlorinated solvents (hexane, toluene, THF, acetone, CH_3CN), either by cooling of saturated solutions or by diffusion methods, produced only glassy oils or amorphous powders.

Infrared spectra of 1: solution, CH_2Cl_2, 2100 (w), 2073 (m), 2065 (m), 2018 (w), 1980 (s), and 1960 (s) cm^{-1}; solid, KBr, 2100 (vw), 2070 (m), and 1940 (vs, br) cm^{-1}. ^{31}P NMR spectra of 1: 310 K, $CDCl_3$, H_3PO_4 ext, δ 20.3 (s, J(W*–P) = 12, 55, 63, 76 Hz); 310 K, acetone-d_6, H_3PO_4 ext, AM_2X pattern, $\delta(P_A)$ = −86.3 (t/d, ^1J(P–P) = 280 Hz, ^2J(P–P) = 23 Hz, J(W–P) = 222 Hz), $\delta(P_M)$ = −3.4 (d/d, ^1J(P–P) = 280, 171 Hz, J(W*–P) = 59, 184, 202 Hz), $\delta(P_X)$ = 230.2 (t/d, ^1J(P–P) = 171, ^2J(P–P) = 23 Hz, J(W–P) = 249 Hz). Coupling assignments for W*–P are discussed in a separate section. Proton NMR spectrum of 1 (270 MHz; $CDCl_3$): δ 5.28 (CH_2Cl_2 of solvation). ^{13}C NMR spectrum (90.6 MHz; $CDCl_3$): δ 193.2 (~20 C, J(W–C) = 124 Hz), 204.9 (~4 C, J(W–C) = 120 Hz).

(6) Scherer, O. J.; Swarowsky, M.; Swarowsky, H.; Wolmershäuser, G. *Angew. Chem., Int. Ed. Engl.* **1988**, *27*, 694. The butadienyl-shaped P_4 ligand of $Rh_2(C_5Me_4Et)_2(CO)(\eta^4\text{-}P_4)$ is η^4-coordinated to one $Rh(C_5Me_4Et)$ fragment and η^2-coordinated to one $Rh(C_5Me_4Et)CO$ fragment. It contains three P–P bonding edges of 2.150 (3), 2.153 (3), and 2.160 (3) Å and one nonbonding edge of 2.697 (3) Å with the $Rh(C_5Me_4Et)CO$ fragment bridging the nonbonding P–P edge. Thermal decarbonylation of this complex produces $[Rh(C_5Me_4Et)(\mu_2\text{-}\eta^2\text{-}P_2)]_2$ (see: Scherer, O. J.; Swarowsky, M.; Wolmershäuser, G. *Angew. Chem., Int. Ed. Engl.* **1988**, *27*, 405).

(7) (a) Barr, M. E.; Adams, B. R.; Weller, R. R.; Dahl, L. F. *J. Am. Chem. Soc.* **1991**, *113*, 3052. (b) Barr, M. E.; Dahl, L. F. *Organometallics*, following paper in this issue.

(8) (a) Hall, M. B.; Fenske, R. F. *Inorg. Chem.* **1972**, *11*, 768. (b) Fenske, R. F. *Prog. Inorg. Chem.* **1976**, *21*, 179. (c) Fenske, R. F. *Pure Appl. Chem.* **1971**, *27*, 61.

(9) He, P.; Avery, J. P.; Faulkner, L. R. *Anal. Chem.* **1982**, *54*, 1313A.

(10) (a) Bjarnason, A.; DesEnfants, R. E.; Barr, M. E.; Dahl, L. F. *Organometallics* **1990**, *9*, 657. (b) Bjarnason, A. *Rapid Commun. Mass Spectrom.* **1989**, *3*, 373.

Attempted Reaction of $W_5(CO)_{24}P_4$ (1) with $P(C_6H_5)_3$. Crystalline 1 (0.05 g) and excess $P(C_6H_5)_3$ (0.10 g) were dissolved in ~30 mL of THF, and the solution was allowed to stir at room temperature overnight. Since no visible reaction had occurred, the solution was then heated to reflux for another 1 h. At the end of this time, a ^{31}P NMR spectrum of the mixture confirmed that no reaction had occurred.

X-ray Crystallographic Determination of $W_5(CO)_{24}P_4 \cdot CH_2Cl_2$ ($1 \cdot CH_2Cl_2$). (a) General Procedures. Intensity data for two different crystal modifications of $1 \cdot CH_2Cl_2$ were collected with graphite-monochromated Mo Kα radiation on a Siemens (Nicolet) P3F diffractometer equipped with a liquid-nitrogen cooling apparatus. Crystal alignment and data-collection procedures are described elsewhere.[11] Crystal data, data-collection parameters, and least-squares refinement parameters for the two different crystal modifications of $1 \cdot CH_2Cl_2$ (under *P4nc* and *I*4 symmetry) are presented in Table I. Cell dimensions and their esd's were obtained for both crystal modifications from least-squares analyses of approximately 20 well-centered reflections ($10° < 2\theta < 20°$). The intensities of three periodically sampled (3/97) standard reflections for each data set did not vary significantly (<±2%) during data collection. The SHELXTL PLUS 4.11 package[12] was used for the structural solution and refinement of $1 \cdot CH_2Cl_2$ in both crystal modifications. Atomic scattering factors for neutral atoms were used together with anomalous dispersion corrections. An empirical ψ-scan absorption correction was applied to both sets of intensity data prior to structural solutions. Patterson maps were used to locate the one independent phosphorus and two independent tungsten atoms, and all other atoms were obtained from difference Fourier syntheses coupled with least-squares refinement.

(b) $W_5(CO)_{24}P_4 \cdot CH_2Cl_2$ ($1 \cdot CH_2Cl_2$) under *P4nc* Symmetry. Crystals suitable for X-ray analysis were grown by the slow cooling of a saturated CH_2Cl_2 solution of 1 to −20 °C. Most crystals were octahedrally or square-pyramidally shaped but were not suitable for analysis due to crystal splitting. An irregularly shaped crystal of approximate dimensions 0.22 × 0.17 × 0.20 mm was mounted on a glass fiber, affixed with epoxy, and coated with paratone-N to exclude air. Axial photographs and a quick data collection based on multiple axial lengths were used to verify the lattice lengths of the chosen tetragonal cell. Intensity-weighted reciprocal lattice plots confirmed the D_{4h}-$4/m2/m2/m$ Laue symmetry; examination of systematic absences indicated the probable space groups to be *P4nc* (C_{4v}, No. 104) and $P4/mnc$ (D_{4h}, No. 128). The mean $|E^2 - 1|$ value of 0.8 and a subsequent successful solution and refinement of the crystal structure confirmed the choice of the noncentrosymmetric space group *P4nc*; attempts at refinement under centrosymmetric $P4/mnc$ symmetry yielded unsatisfactory results. The origin was defined in the *c* direction by an arbitrary selection of $z = {}^1/_4$ for the W atom on the 4-fold axis. Positional parameters for the carbon atom of the crystallographically 4-fold-disordered CH_2Cl_2 molecule and its isotropic thermal parameter were fixed during refinement. Hydrogen atoms were omitted from the solvent molecule. All atoms of 1 and the two Cl atoms of the solvent molecule were refined anisotropically. The final difference Fourier map displayed several residual electron density peaks of <3.0 e/Å^3 at physically nonmeaningful locations near the W atoms but no other unusual features. Due to the space-group polarity in the *c* direction, a separate refinement with inverted atomic coordinates was carried out; this refinement produced a slightly higher $R_1(F)$ value.

Atomic coordinates from the final least-squares cycle are listed in Table II. Selected interatomic distances and bond angles are presented in Table III. Tables of the anisotropic displacement coefficients for all atoms and of observed and calculated structure factor amplitudes are available as supplementary material.

(c) $W_5(CO)_{24}P_4 \cdot CH_2Cl_2$ ($1 \cdot CH_2Cl_2$) under *I*4 Symmetry. A number of the crystals, grown as described above, were found from an X-ray analysis to have a body-centered tetragonal unit cell with a unit cell volume virtually identical to that of the primitive *P4nc* cell. A square-pyramidal-shaped crystal of dimensions 0.23 × 0.23 × 0.17 mm was mounted for data collection as described above. Data collection parameters for this crystal are listed in Table I. Axial photographs and the intensity-weighted reciprocal lattice data pointed to C_{4h}-$4/m$ Laue symmetry; systematic absences of *hkl* for $h + k + l$ odd indicated the probable space groups to be *I*4 (C_4, No. 79), $I\bar{4}$ (S_4, No. 82), and $I4/m$ (C_{4h}, No. 87). Successful solution and refinement confirmed the final choice of space group *I*4. Attempted refinement under centrosymmetric $I4/m$ symmetry was much less satisfactory; this refinement gave rise to severe elongation of the thermal ellipsoids of the equatorial tungsten atoms on the mirror plane, and difficulties were encountered in locating and refining the carbonyl groups. Since an ordered structure under *I*4 symmetry gave a large residual peak on the 4-fold axis within a W–P bonding distance from the P_4 ring, each molecular unit was then modeled with an occupancy factor of 75% for the primary orientation and an occupancy factor of 25% for an inverted orientation in which the molecule is mirrored across the plane of the four phosphorus atoms. The

Table II. Atomic Coordinates (×10^4) and Equivalent Isotropic Displacement Coefficients[a] (Å^2 × 10^3) for $W_5(CO)_{24}P_4 \cdot CH_2Cl_2$ ($1 \cdot CH_2Cl_2$) under *P4nc* Symmetry

	x	y	z	U(eq)
W(1)	7253 (1)	1624 (1)	4258 (2)	51 (1)
W(2)	10000	0	2500	34 (1)
P(1)	8912 (5)	590 (5)	3902 (5)	39 (2)
C(1)	6016 (24)	2551 (20)	4557 (37)	104 (7)
O(1)	5244 (17)	3108 (19)	4771 (21)	96 (6)
C(2)	6524 (25)	1230 (31)	3011 (27)	80 (7)
O(2)	6153 (30)	948 (25)	2326 (25)	156 (7)
C(3)	7961 (35)	1981 (25)	5467 (18)	79 (7)
O(3)	8266 (41)	2165 (38)	6073 (28)	209 (8)
C(4)	7928 (28)	2970 (26)	3614 (28)	77 (7)
O(4)	8282 (26)	3674 (20)	3270 (23)	109 (7)
C(5)	6508 (36)	407 (29)	4789 (43)	159 (8)
O(5)	6099 (27)	−392 (23)	5140 (32)	177 (8)
C(6)	11336 (29)	528 (21)	1837 (19)	62 (6)
O(6)	12183 (19)	832 (22)	1556 (25)	117 (7)
Cl(1)	10000	0	6153 (14)	110 (5)
Cl(2)[b]	11314 (34)	−173 (32)	7604 (38)	124 (8)
C(7)	10000	0	7300	200

[a] The equivalent isotropic *U* is defined as one-third the trace of the orthogonalized U_{ij} tensor. [b] The site occupancy factor for Cl(2), which is crystal-disordered in four equivalent positions around the C_4 axis, is fixed at 0.25.

Table III. Selected Interatomic Distances and Bond Angles for $W_5(CO)_{24}P_4 \cdot CH_2Cl_2$ ($1 \cdot CH_2Cl_2$) under *P4nc* Symmetry

Interatomic Distances (Å)			
W(1)–P(1)	2.441 (6)	W(1)–C(1)	1.935 (29)
W(1)–C(2)	2.073 (37)	W(1)–C(3)	2.003 (30)
W(1)–C(4)	2.063 (34)	W(1)–C(5)	1.904 (43)
W(2)–P(1)	2.533 (7)	W(2)–C(6)	1.999 (32)
C(1)–O(1)	1.203 (38)	C(2)–O(2)	1.145 (51)
C(3)–O(3)	0.981 (51)	C(4)–O(4)	1.083 (44)
C(5)–O(5)	1.207 (55)	C(6)–O(6)	1.172 (42)
P(1)–P(1B)	2.137 (8)	Cl(1)–C(7)	1.664 (20)
Cl(2)–C(7)	1.676 (42)		
Bond Angles (deg)			
P(1)–W(1)–C(1)	175.2 (8)	P(1)–W(1)–C(2)	92.9 (9)
P(1)–W(1)–C(3)	86.5 (11)	P(1)–W(1)–C(4)	89.1 (10)
P(1)–W(1)–C(5)	94.5 (13)	W(1)–C(1)–O(1)	177.7 (41)
W(1)–C(2)–O(2)	175.6 (31)	W(1)–C(3)–O(3)	176.7 (45)
W(1)–C(4)–O(4)	179.6 (37)	W(1)–C(5)–O(5)	175.9 (44)
C(1)–W(1)–C(2)	89.8 (17)	C(1)–W(1)–C(3)	90.8 (18)
C(2)–W(1)–C(3)	179.1 (14)	C(1)–W(1)–C(4)	87.0 (14)
C(2)–W(1)–C(4)	87.7 (15)	C(3)–W(1)–C(4)	92.9 (14)
C(1)–W(1)–C(5)	89.6 (16)	C(2)–W(1)–C(5)	88.1 (21)
C(3)–W(1)–C(5)	91.3 (20)	C(4)–W(1)–C(5)	174.6 (19)
P(1)–W(2)–C(6)	136.2 (8)	P(1)–W(2)–P(1A)	73.2 (3)
P(1)–W(2)–P(1B)	49.9 (2)	P(1)–W(2)–C(6A)	92.8 (9)
P(1B)–W(2)–P(1C)	73.2 (3)	W(2)–C(6)–O(6)	171.5 (28)
C(6)–W(2)–P(1B)	141.9 (9)	C(6)–W(2)–C(6A)	122.5 (17)
P(1A)–W(2)–C(6A)	136.2 (8)	C(6)–W(2)–C(6B)	76.6 (7)
W(1)–P(1)–W(2)	138.8 (3)	P(1B)–P(1)–P(1C)	90.0 (1)
W(1)–P(1)–P(1B)	137.0 (3)	W(2)–P(1)–P(1B)	65.1 (1)
W(1)–P(1)–P(1C)	130.4 (3)	Cl(1)–C(7)–Cl(2)	105.3 (19)

(11) Byers, L. R.; Dahl, L. F. *Inorg. Chem.* **1980**, *19*, 277.
(12) SHELXTL PLUS 4.11. Siemens Analytical X-Ray Instruments, Inc., 600 Enterprise Lane, Madison, WI 53719-1173.

actual refinement parameters listed in Table I are based upon a partially modeled crystal disorder in which the primary orientation (75%) was allowed to refine without constraints and only the apical W atom of the inverted orientation (25%) was included. Since the secondary orientation of 1 is superimposed upon the anticipated location of a CH_2Cl_2 molecule of solvation, the solvent molecule was not included in this model. The tungsten and phosphorus atoms were then refined anisotropically and the carbonyl atoms refined isotropically with no constraints upon their positional and thermal parameters. The final refinement yielded molecular parameters reasonably similar to those obtained from the crystal data for the crystal-ordered 1 in the tetragonal unit cell with *P4nc* symmetry. A more extensive modeling of this crystal disorder requires that each of the two disordered orientations be restrained as fixed, rigid groups because spatial overlap of the equatorial carbonyl ligands of the $W(CO)_5$ groups for the two orientations precludes refinement of positional coordinates. Due to the pseudosymmetric nature of the crystal disorder, no unambiguous preference of enantiomers was observed from a separate least-squares refinement which gave a slightly higher $R_1(F)$ value for the inverted atomic coordinates. All crystallographic structural information presented is from the more precise refinement of the *P4nc* crystal, but all spectral data are from the bulk mixture of the primitive and body-centered crystalline material.

Tables of atomic coordinates, selected interatomic distances and bond angles, anisotropic displacement coefficients for all atoms, and observed and calculated structure factor amplitudes of $1{\cdot}CH_2Cl_2$ under *I*4 symmetry are available as supplementary material.

Nonparametrized Fenske–Hall Molecular Orbital Calculations. All calculations were performed with the Fenske–Hall molecular orbital model.[8] This nonparametrized model is based on a self-consistent-field (SCF) method, which is an approximation of the Hartree–Fock–Roothaan procedure. The resulting eigenvectors and eigenvalues are completely determined by the atomic basis sets and the geometry of the molecule used. All atomic positions were generated from the orthogonalized coordinates of 1 obtained from the structural determination under *P4nc* symmetry. Basis functions[13] used were for neutral atoms.

Calculations for the hypothetical $W(CO)_4P_4$ molecule were carried out on transformed (atomic to molecular) orbital basis sets on the $W(CO)_4$ fragment combined with the bare P_4 ring. Calculations were also performed for the entire molecule (1) by appropriate combinations of the P_4, $W(CO)_4$, and four $W(CO)_5$ fragments under C_4-4 symmetry.

Results and Discussion

Crystal and Molecular Structural Features of $W_5(CO)_{24}P_4{\cdot}CH_2Cl_2$ ($1{\cdot}CH_2Cl_2$). The independent unit of $1{\cdot}CH_2Cl_2$ under *P4nc* symmetry consists of a single phosphorus atom coordinated to one $W(CO)_5$ fragment and to one-fourth of a $W(CO)_4$ fragment, which sits on the principal C_4 axis. The resulting molecular configuration of C_4 symmetry consists of an apical $W(CO)_4$ group coordinated to a bonding phosphorus ring of four crystallographically equivalent P–$W(CO)_5$ groups. A CH_2Cl_2 molecule of solvation lies below the phosphorus ring with the carbon and one chlorine atom located on the C_4 axis and with the other Cl atom being disordered in four equivalent positions around this axis. The Cl atom on the C_4 axis is not within bonding distance of the phosphorus ring (Cl···P = 3.597 Å). Figure 1 presents an ORTEP diagram and the labeling scheme for the independent atoms of 1 and the CH_2Cl_2 molecule of solvation. The tetragonal unit cell under *P4nc* symmetry contains two $1{\cdot}CH_2Cl_2$ formula species, which pack with no unusually short intermolecular contacts.

While the nature of the presumed crystallographic disorder of $1{\cdot}CH_2Cl_2$ under *I*4 symmetry would necessarily obscure a CH_2Cl_2 molecule of solvation, the similarity of its unit cell volume to that of the primitive unit cell under *P4nc* symmetry stongly suggests that the solvent molecule is also present in the body-centered cell. In fact, the observation that the two crystal forms cocrystallize is consistent with there being similar packing forces in the ordered *P4nc* and crystal-disordered *I*4 cells. Figure 2 illustrates the difference in packing for these two crystal forms.

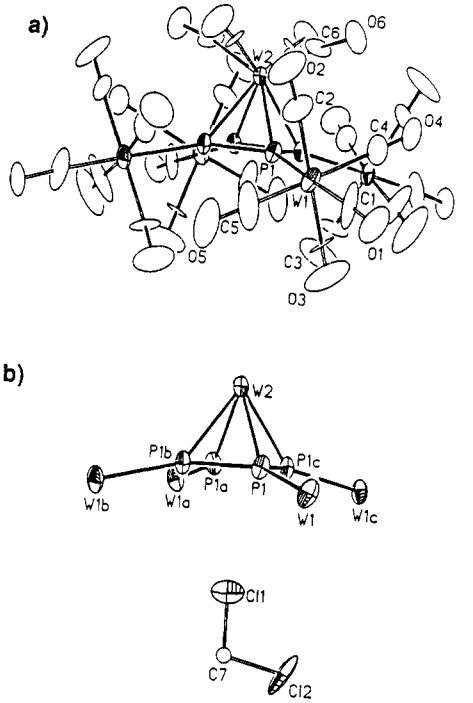

Figure 1. (a) Molecular configuration of $W_5(CO)_{24}P_4$ (1), which possesses C_4-4 crystallographic site symmetry in the tetragonal unit cell of *P4nc* symmetry. Only the crystallographically independent atoms of the molecule are labeled. In this C_4-averaged structure, the apical W(2) atom of the $W(CO)_4$ fragment lying on the crystallographic 4-fold axis is linked to the four symmetry-related basal P(1) atoms of a square P_4 ring. The unshared electron pair of each basal P(1) atom is additionally bonded to the W(1) atom of a Lewis-acid $W(CO)_5$ ligand. (b) The $W(PW)_4$ framework of 1 with the CH_2Cl_2 molecule of solvation. One of the two chlorine atoms, Cl(1), and the carbon atom, C(7), of the dichloromethane molecule lie on the crystallographic 4-fold axis such that the chlorine atom sterically occupies an octahedal-like nonbonding site adjacent to the $W(PW)_4$ core. The other chlorine atom, Cl(2), is crystallographically disordered by the 4-fold axis over four positions, of which only one site is shown in (b). All thermal ellipsoids are drawn at the 30% probability level.

Electron-Counting Analysis of $W_5(CO)_{24}P_4$ (1). The square-pyramidal WP_4 core, possessing five vertices and eight bonds, requires 34 localized valence electrons.[14] This electron count is achieved for 1 by contributions of five valence electrons from each phosphorus atom and fourteen electrons from the apical $W(CO)_4$ group. The four Lewis-acid $W(CO)_5$ adducts coordinated to the phosphorus atoms contribute no electrons to the WP_4 core. The independent $(CO)_4W$–P distance of 2.533 (7) Å corresponds to a normal π-bonding value, but the mean $(CO)_5W$–P distance of 2.441 (6) Å is approximately 0.1–0.2 Å shorter than σ-bonding distances in analogous complexes.[15-17] The

(13) Clementi, E.; Ramondi, D. L. *J. Chem. Phys.* **1963**, *38*, 2686.

(14) (a) Wade, K. *Adv. Inorg. Radiochem.* **1976**, *18*, 1. (b) Wade, K. *J. Chem. Soc., Chem. Commun.* **1971**, 792. (c) Mingos, D. M. P. *Acc. Chem. Res.* **1984**, *17*, 311. (d) Mingos, D. M. P. *Nature (London), Phys. Sci.* **1972**, *236*, 99. (e) Lauher, J. W. *J. Am. Chem. Soc.* **1978**, *100*, 5305.

(15) (a) Holand, S.; Mathey, F.; Fischer, J. *Polyhedron* **1986**, *5*, 1413. (b) Bartsch, R.; Hitchcock, P. B.; Nixon, J. F. *J. Organomet. Chem.* **1988**, *340*, C37.

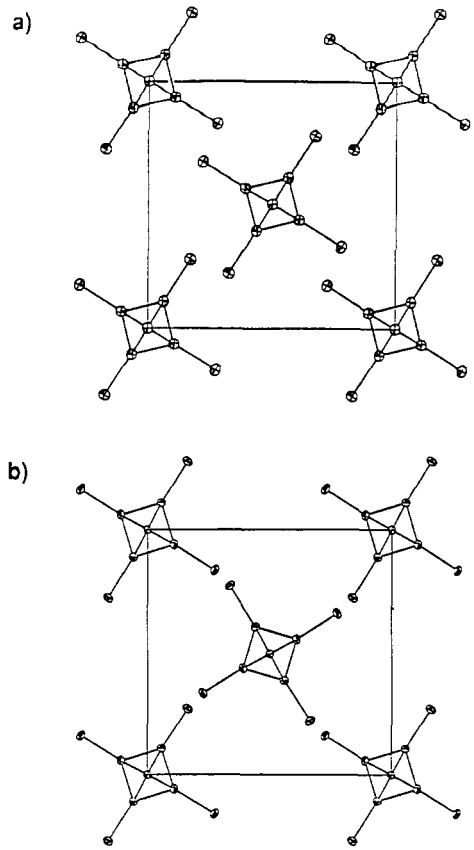

Figure 2. Packing diagrams for the different tetragonal unit cells of $W_5(CO)_{24}P_4$ (1) viewed along the c axis: (a) body-centered cell ($I4$) in which the two molecules per cell are related by the I-centered translation; (b) primitive cell ($P4nc$) in which the two molecules per cell are related by a glide-plane symmetry operation. The carbonyl ligands and CH_2Cl_2 molecules of solvation are omitted. In each of these unit cells, the square-pyramidal $W(PW)_4$ fragment of crystallographic C_4 site symmetry ideally possesses C_{4v}-$4mm$ symmetry. Inclusion of the carbonyl ligands lowers the symmetry to the required C_4 due to the equatorial carbonyl ligands of the four basal $W(CO)_5$ fragments being rotationally twisted from a C_{4v} configuration.

independent P–P distance of 2.137 (8) Å in the P_4 ring of 1 is similar to the average distance of 2.16 Å found in the P_4 ring of $NbCp^*(CO)_2P_4$ (2).[5]

Spectral–Electrochemical Properties of $W_5(CO)_{24}P_4$ (1). (a) Infrared Spectral Analysis. Infrared spectra of $1{\cdot}CH_2Cl_2$ exhibit carbonyl absorption patterns characteristic of the one $W(CO)_4$ and four $W(CO)_5$ fragments of the molecule. A solution infrared spectrum in CH_2Cl_2 shows five distinct terminal carbonyl peaks. A solid-state IR spectrum (KBr pellet) is similar, but less well-resolved, with three absorption maxima in the terminal carbonyl region.

(b) Mass Spectral Analysis. The high-mass region of the positive-ion spectrum (Figure 3) primarily contains ion-peak envelopes for the parent-ion $W_5(CO)_{24}P_4^+$ (m/z ~1714) and for ions corresponding to the loss of one and two $W(CO)_5$ fragments, respectively (m/z ~ 1390, 1067). The negative-ion spectrum (Figure 3) contains a number of high-mass ion peaks, which are related to the parent-ion peak by the loss of carbonyl ligands. The ion-fragment $W(CO)_4P_4^-$ (m/z ~420) is the smallest identified molecular fragment that potentially contains an intact P_4 ring. The

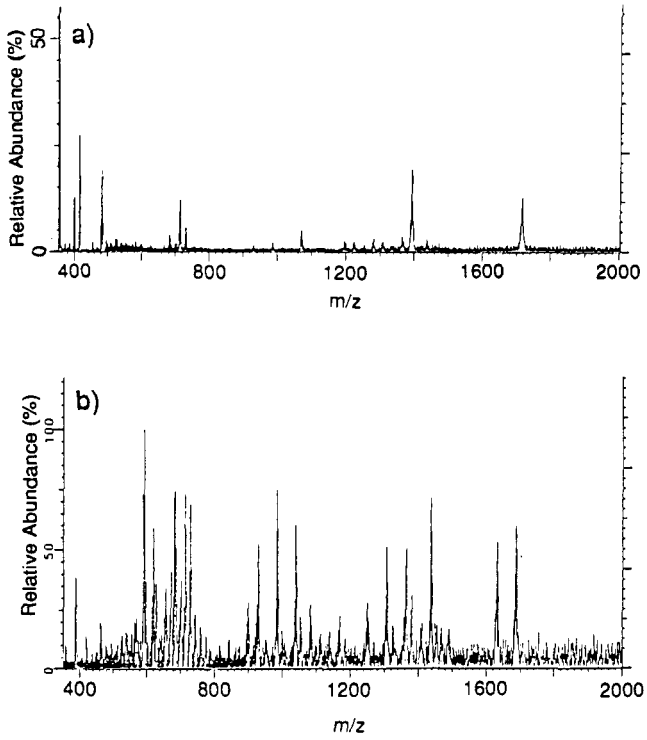

Figure 3. (a) Positive-ion and (b) negative-ion LD/FT mass spectra for $W_5(CO)_{24}P_4$ (1).

$W(CO)_6^{+,-}$ ions were the most abundant ion fragments produced in the positive- and negative-ion LD/FT mass spectra, respectively, and $W(CO)_6^+$ was the highest mass ion detected in a standard room-temperature EI mass spectrum. Other relatively low-mass positive- and negative-ion peaks are assigned to tungsten carbonyls and to additional monomeric and dimeric fragments, some of which contain chlorine atoms which presumably originate from the CH_2Cl_2 molecule of solvation. A full table of ion-peak assignments for the positive- and negative-ion LD/FT mass spectra of 1 is available as supplementary material.

(c) Electrochemical Analysis. Cyclic voltammograms for 1 do not exhibit any reversible redox couples within the observed range for each solvent (THF, +1.0 to −2.0 V; CH_2Cl_2, +1.8 V to −1.0 V). 1 shows irreversible reduction waves at ca. −1.42 V in THF and at ca. −0.65 V in CH_2Cl_2.

(d) Solution and Solid-State ^{31}P NMR Analysis and Resulting Structural Interpretation. Solution ^{31}P NMR spectra provide highly informative data concerning the nature of the P_4 ring in $W_5(CO)_{24}P_4$ (1). In low-polarity solvents ($CHCl_3$, CH_2Cl_2, C_6H_6), the four phosphorus atoms of the ring are equivalent at room temperature on an NMR time scale. Under these conditions, a ^{31}P NMR spectrum (202.5 MHz; 310 K; $CDCl_3$; 85% H_3PO_4 ext) of 1 exhibits a very sharp singlet ($w_{1/2}$ = 2.6 Hz) at δ 20.3 ppm. This singlet peak displays four sets of doublet couplings: one narrow set with J = 12 Hz and three broad, low-resolution sets with J = 55, 63, and 76 Hz, all in intensity ratios (~1:14:1) consistent with ^{31}P coupling to ^{183}W. In previously reported structures containing W coordinated to the π orbitals of P_n or $P_m(CR)_n$ ($m + n = 5$) rings,[13,14] no π-bonded W–P couplings were detected. Thus, while each phosphorus atom in 1 is bonded to two tungsten atoms, each P nucleus may be magnetically coupled to just its one σ-bonded equatorial tungsten adduct. Even the larger coupling constants of 55, 63, and 76 Hz, however, are much smaller than σ-coordinated ^1J(W–P) coupling constants of 130–220 Hz found in nonfluxional tungsten–phosphorus

(16) Scherer, O. J.; Schwalb, J.; Swarowsky, H.; Wolmershäuser, G.; Kaim, W.; Gross, R. *Chem. Ber.* **1988**, *122*, 443.
(17) Driess, M.; Fanta, A. D.; Powell, D. R.; West, R. *Angew. Chem., Int. Ed. Engl.* **1989**, *28*, 1038.

complexes.[13,15] Some of the couplings found in this room-temperature spectrum could be ^1J(P–P) or ^2J(P–P) couplings; when any one of the equivalent phosphorus atoms is coordinated to an NMR-active ^{183}W, the ring symmetry is reduced and the phosphorus atoms become magnetically inequivalent. Due to the low solubility of **1** in $CDCl_3$ and to the low resolution of the doublet sets, additional information concerning the specific designation of coupling constants could not be obtained from ^{31}P COSY NMR spectral experiments.

A low-temperature-solution ^{31}P NMR spectrum (202.5 MHz; 243 K; CD_2Cl_2; 85% H_3PO_4 ext) presents a time-resolved picture of the P_4 ring in **1**. Three resonance signals that correspond to an AM_2X pattern are observed for the four phosphorus nuclei: $\delta(P_A)$ = −89.8 ppm (t/d, J(P–P) = 280/28 Hz), $\delta(P_M)$ = −3.1 ppm (d/d, J(P–P) = 280, 170 Hz), and $\delta(P_X)$ = 226.6 ppm (t/d, J(P–P) = 170/28 Hz). Since the solubility of **1** is greatly reduced at low temperatures, the quality of this low-temperature spectrum is adversely affected both by decreased concentrations of **1** and by the resultant increased turbidity of the sample solution.

Room-temperature ^{31}P NMR spectra of **1** in strongly polar solvents (acetone, CH_3CN, DMSO) are nearly identical to the low-temperature ^{31}P spectrum of **1** in CH_2Cl_2. Under these conditions, a ^{31}P NMR spectrum (202.5 MHz; 310 K; acetone-d_6; 85% H_3PO_4 ext) displays the same AM_2X pattern as well as resolved couplings of ^{31}P with ^{183}W: $\delta(P_A)$ = −86.3 ppm (t/d, ^1J(P–P) = 280, ^2J(P–P) = 23 Hz, J(W–P) = 222 Hz), $\delta(P_M)$ = −3.4 ppm (d/d, ^1J(P–P) = 280, 171 Hz, J(W*–P) = 59, 184, 202 Hz), and $\delta(P_X)$ = 230.2 ppm (t/d, ^1J(P–P) = 171, ^2J(P–P) = 23 Hz, J(W–P) = 249 Hz). The couplings denoted as W*–P are assigned as follows. The smallest coupling of 59 Hz is presumably a P_M–$P_{M'}$ two-bond coupling as found for P_A–P_X (23 Hz); symmetry reduction of M_2 to M and M′ occurs when one of these two nuclei is coupled to the NMR-active ^{183}W. The two larger couplings of 184 and 202 Hz may be either two ^1J(W–P) couplings to the σ- and π-bonded W atoms or one ^1J(W–P) and one ^2J(W–P) between the P_M nuclei and the σ-bonded $W(CO)_5$ groups. Given the previous absence of observed π-bonded W–P coupling, the latter interpretation is more probable.

Solid-state ^{31}P NMR spectra were collected on both crystalline and amorphous samples in an attempt to elucidate the solid-state configuration of the P_4 ligand; however, poor resolution of the spectral data precludes extraction of any definitive information about the *cyclo*-P_4 bonding. A room-temperature solid-state ^{31}P NMR spectrum (121.4 MHz) of microcrystalline $W_5(CO)_{24}P_4$ (**1**) with the CH_2Cl_2 molecule of solvation present exhibits two broad signals ($w_{1/2} \sim$ 8800 Hz) of approximately equal intensities—viz., one at δ 23 ppm (similar to the chemical shift found in the room-temperature $CHCl_3$ solution spectrum) and one at δ 52 ppm. While the four phosphorus nuclei of **1** could potentially exist as two magnetically inequivalent sets of two nuclei each under these experimental conditions, both the A_2B_2 pattern and the minimal difference in chemical shift values are inconsistent with the resolved solution NMR data. Therefore, it is more likely that the observed pattern for the four nuclei is composed of two ^{31}P singlets whose chemical shift differences arise from packing variations between the two nonseparated crystal forms of **1**·CH_2Cl_2 with tetragonal primitive *P4nc* and body-centered *I*4 unit cells. If this is the case, then the two crystal forms of **1**·CH_2Cl_2 are present in approximately equal amounts. Solid-state ^{31}P NMR spectra of amorphous **1** from acetone are not particularly informative due to poor signal resolution. A room-temperature spectrum shows a very broad ($w_{1/2}$ = 37 000 Hz), unresolved double hump centered at approximately 30 ppm, which does not change significantly in a spectrum obtained at low temperature (180 K). The extremely broad signals and poor resolution are presumably due to the multitude of electronic environments that **1** experiences in an amorphous solid state as well as to the usual line-broadening causes such as dipole–dipole interactions and chemical shift anisotropy. Solid-state and solution ^{31}P NMR spectra are available as supplementary material.

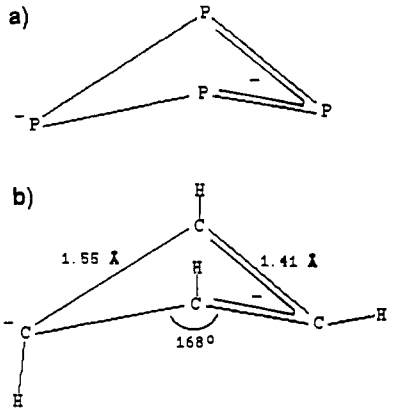

Figure 4. Presumed C_s-*m* kite-shaped bonding configuration which may be considered as the composite of an allyl-like anion and a localized anion for (a) a hypothetical *cyclo*-P_4^{2-} dianion and (b) the electronically equivalent hypothetical $C_4H_4^{2-}$ ring. The bond lengths and angles and approximate positions of the hydrogen atoms in the cyclobutadienyl dianion were obtained from an ab initio vibrational analysis.[33]

A solution ^{1}H NMR spectrum (270 MHz; $CDCl_3$) of **1**·CH_2Cl_2 shows only the hydrogen atoms of the CH_2Cl_2 solvent molecule at δ 5.28 ppm. Solid-state ^{1}H NMR (300 MHz) data for microcrystalline **1**·CH_2Cl_2 display two signals of equal intensity, presumably from the hydrogens of the methylene chloride, which confirms that this solvent molecule is present in a crystalline sample. A room-temperature solution ^{13}C NMR spectrum (90.6 MHz; $CDCl_3$) of **1**·CH_2Cl_2 exhibits two carbonyl carbon signals—viz., a large one at δ 193.2 ppm (J(W–C) = 124 Hz) assigned to the 20 carbonyl carbon atoms of the four equatorial $W(CO)_5$ adducts and a smaller one at δ 204.9 ppm (J(W–C) = 120 Hz) assigned to the 4 carbonyl carbon atoms of the apical $W(CO)_4$ fragment.

Discussion

Figure 4 presents a proposed bonding configuration for the *cyclo*-P_4 ligand in **1**. This ligand of pseudo-mirror-plane symmetry may be formally considered as a P_4^{2-} ring which consists of an allyl-like P_3^- monoanion coordinated to a fourth atomic P^- anion. This C_s kite-shaped geometry is one of the two models suggested by Scherer et al.[5] for the *cyclo*-P_4 ligand in $NbCp^*(CO)_2P_4$ (**2**). Their crystallographic analysis of **2** revealed a slight distortion of the P_4 ring from a square to a planar kite-shaped configuration with two shorter P–P distances of 2.141 (2) and 2.136 (2) Å and two longer P–P distances of 2.178 (2) and 2.181 (2) Å. While this distortion is consistent with the AMX_2 pattern of three well-resolved signals observed in a low-temperature ^{31}P NMR spectrum of this compound, the pseudo-mirror-plane symmetry of **2** led to the proposal by Scherer et al.[5] that the nonequivalency of the P nuclei could be induced by hindered ring rotation of the *cyclo*-P_4 ligand. However, the AM_2X pattern of the three ^{31}P resonances for the P_4 ring of **1**, which has 4-fold coordinative symmetry, cannot be explained in this fashion.

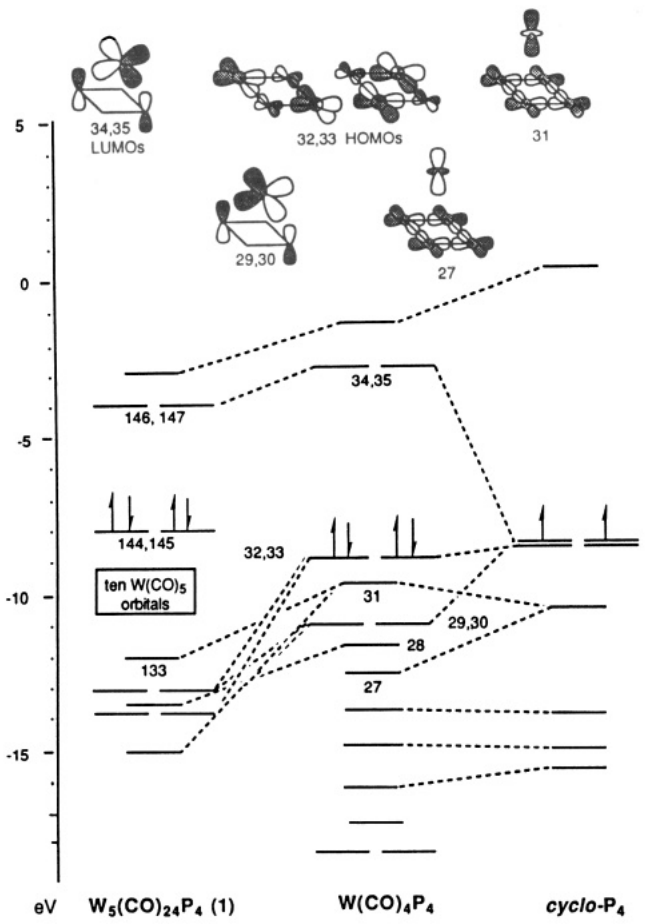

Figure 5. Correlation diagram for selected MOs of $W_5(CO)_{24}P_4$ (1) under C_4 symmetry. These MOs (shown at the far left) are appropriate combinations of the $W(CO)_4P_4$ MOs, shown in the middle, and those of the four $W(CO)_5$ fragments (not shown). MOs of the P_4 ring are shown at the far right. The 12 highest energy occupied orbitals (including the HOMOs) of 1 are primarily composed of W $5d_{xz}$ and $5d_{yz}$ AOs of the four $W(CO)_5$ fragments. The HOMO/LUMO gap is 3.96 eV.

This kite-shaped C_s model of the *cyclo*-P_4 ligand may be visualized as possessing four equivalent charge-localized states with four transition states between them. Rapid exchange between the lower energy charge-localized states results in a time-averaged structure in which the four phosphorus nuclei are essentially equivalent. Since the rate of ring fluctuation at room temperature is observed to be slower in strongly polar solvents than in less polar solvents, solvent molecules apparently influence the electronic distribution around the phosphorus ring and subsequently raise the energy barrier between each equivalent thermodynamically favored C_s configuration. Since 1 has no Lewis-acid sites available for direct coordination with the highly polar, Lewis-base solvents, these solvent molecules most probably affect ring electronic distribution via polar stabilization of the charge-localized kite-shaped configuration.

The attempted reaction of 1 with $P(C_6H_5)_3$ had two goals. Primarily, it was hoped that $P(C_6H_5)_3$ would strip the $W(CO)_5$ adducts from 1 to produce a bare *cyclo*-P_4 unit, as in **2**. Secondly, CO replacement by $P(C_6H_5)_3$, and subsequent breaking of the C_4 molecular symmetry, was deemed desirable for further crystallographic and spectral studies. Although the experimental conditions were relatively mild, the complete absence of any reaction of 1 with $P(C_6H_5)_3$ suggests that neither the CO ligands nor the $W(CO)_5$ adducts of 1 are particularly labile.

Structural–Bonding Analysis of $W_5(CO)_{24}P_4$ (1). In many of the organometallic polyphosphido complexes synthesized and characterized by Scherer and co-workers,[16,18,19] the metal-complexed P_5 and P_6 rings exhibit a planarity and similarity of P–P bond lengths consistent with electron-delocalized bonding schemes as formulated for analogous "aromatic" hydrocarbon rings; in other structures,[5,16] these rings exhibit small, discernible differences in specific P–P and M–P bond lengths, which indicate a more localized bonding picture. All of these polyphosphorus ligands, however, are virtually planar.

Complexation of an apical metal fragment to the π orbitals of the *cyclo*-P_4 ligand may be described from a valence bond viewpoint in terms of an oxidation-state formalism. In the case of 1, the resulting electronic configuration may be regarded as an intermediate between a d^4 W(II) $W(CO)_4^{2+}$ fragment interacting with a *cyclo*-P_4^{2-} ligand and a neutral W(0) $W(CO)_4$ fragment interacting with a *cyclo*-P_4 ligand. In light of the qualitative bonding comparisons made between dimetal complexes containing *cyclo*-P_n bridging rings (n = 5, 6) and traditional "triple-decker" sandwich complexes containing analogous hydrocarbon rings,[4,20] it appears reasonable that the *cyclo*-P_4 ligand[21–25] can be related to the electronically equivalent *cyclo*-C_4R_4 ligand[26–30] and the hybrid *cyclo*-[1,3-$(PCR)_2$]

(18) Scherer, O. J.; Sitzmann, H.; Wolmershäuser, G. *Angew. Chem., Int. Ed. Engl.* **1985**, *24*, 351.
(19) Scherer, O. J.; Brück, T.; Wolmershäuser, G. *Chem. Ber.* **1988**, *121*, 935.
(20) Gimarc, B. M. *Pure Appl. Chem.* **1990**, *62*, 423.
(21) Gaseous P_4 molecules were shown from electron diffraction measurements[22] and vibrational–rotational Raman spectroscopy[23] to possess a regular tetrahedral T_d configuration with a P–P bond length of 2.22 Å. Ab initio quantum mechanical calculations[24] not only have reproduced the experimentally determined ground-state geometry but also have provided reliable estimates of the ionization potentials, ^{31}P NMR shielding constants, and the dissociation energy of P_4. Both of the two stable crystal forms of white phosphorus (hexagonal α-form below and cubic β-form at −77 °C (1 atm) to melting point) consist of tetrahedral P_4 molecules.[25] Recent calculations[24] of P_4 via a density functional method combined with molecular dynamics and simulated annealing techniques indicated that, in addition to the most stable tetrahedral P_4 structure, two other stable P_4 structures also corresponded to local minima in the energy surface. These less stable structures consist of a "roof" C_{2v} configuration which is 2.19 eV above the T_d structure and 0.60 eV more stable than the planar rectangular D_{2h} configuration with bond lengths of 2.06 and 2.27 Å.[24]
(22) Maxwell, L. R.; Hendricks, S. B.; Mosley, V. M. *J. Chem. Phys.* **1935**, *3*, 699.
(23) Brassington, N. J.; Edwards, H. G. M.; Long, D. A. *J. Raman Spectrosc.* **1981**, *11*, 346.
(24) For a comprehensive theoretical–experimental comparison of structures and vibrational frequencies of isomers of P_4 and other phosphorus clusters in their ground and low-lying excited states, see: Jones, R. O.; Hohl, D. *J. Chem. Phys.* **1990**, *92*, 6710, and references cited therein.
(25) Donahue, J. *The Structures of the Elements*; John Wiley and Sons, Inc.: New York, 1974; Chapter 8, pp 296–299 and references cited therein.
(26) Accumulated experimental and theoretical investigations[27] have provided a mutually consistent conclusion that "free" *cyclo*-C_4H_4 possesses a singlet ground state of rectangular D_{2h} geometry with localized double and single C–C bonds. This current conclusion is in complete harmony with analogous rectangular D_{2h} ring geometries determined for several substituted cyclobutadienes from X-ray crystallographic analyses.[28] It is noteworthy that recent spectroscopic data indicate a dynamic interconversion of the two rectangular D_{2h} valence tautomeric forms of cyclobutadiene (i.e., a bond-switching process) via heavy-atom tunneling in which the transition state has a square-planar D_{4h} configuration with a C–C distance of ca. 1.44 Å.[27f]
(27) For recent comprehensive theoretical and/or experimental reviews involving cyclobutadiene, see: (a) Bally, T.; Masamune, S. *Tetrahedron* **1980**, *36*, 343. (b) Borden, W. T.; Davidson, E. R. *Acc. Chem. Res.* **1981**, *14*, 69. (c) Lloyd, D. *Non-Benzenoid Conjugated Carbocylic Compounds*; Elsevier: New York, 1984; pp 197–204. (d) Maier, G. *Angew. Chem., Int. Ed. Engl.* **1988**, *27*, 309. (e) Michl, J.; Bonacic-Koutecky, V. *Electronic Aspects of Organic Photochemistry*; Wiley Press: New York, 1990. (f) Arnold, B. R.; Michl, J. Spectroscopy of Cyclobutadiene. In *Kinetics and Spectroscopy of Carbenes and Biradicals*; Platz, M. S., Ed.; Plenum Press: New York, 1991; Chapter 1, pp 1–34.

ligand.[31,32] An ab initio vibrational analysis[33] of the cyclobutadiene dianion showed that a slightly puckered C_s allylic "kite" configuration (dihedral angle = 168°) is favored for the noncoordinated system (Figure 4). In an electronically equivalent P_4^{2-} ring system, nonbonding electron pairs would replace the C–H bonding pairs. In $NbCp^*(CO)_2P_4$ (**2**), the positions of the nonbonding electron pairs of the P_4 ring are not discernible. In **1**, however, the equatorial $W(CO)_5$ groups may be used to examine the preferred configuration of the ring substituents. If the $W(CO)_5$ adducts were staggered, as is suggested for the hydrogen atoms of the noncoordinated $C_4H_4^{2-}$ dianion, one would expect to observe severe elongation along the *c* direction of the anisotropic thermal ellipsoids of the coordinated tungsten atoms and their carbonyls in the crystallographically averaged structure of **1**. No such systematic elongation of the atomic thermal ellipsoids is apparent. Crystallographically, the equatorial tungsten atoms are located ca. 17.0° below the plane of the P_4 ring, away from the apical $W(CO)_4$ group. The symmetry-equivalent bending of the four $W(CO)_5$ substituents exo to the apical W atom is analogous to nonplanar exo deformations of the ring substituents of metal-coordinated cyclobutadiene rings normally found in cyclobutane–metal complexes. This exo-substituent bending angle in metal–C_4R_4(ring) systems has been explained from orbital overlap considerations (with assumed absence of steric effects which would also favor the exo configuration) in terms of ring carbon-2p orbital reorientations providing better bonding interactions with the d_π metal orbitals.[34]

The possible existence of any puckering of the P_4 ring in **1** would be impossible to detect due to its crystallographically averaged structure of C_4 site symmetry. Moreover, the four crystallographically independent phosphorus atoms of the P_4 ring in **2** are reported to be coplanar.[5]

While the low-energy configuration of the *cyclo*-P_4 unit of **1** does appear to be consistent with one predicted structure of $C_4H_4^{2-}$, other more recent calculations[35] have indicated that the kite-shaped C_s-*m* geometry does *not* correspond to an energy minimum for the isolated $C_4H_4^{2-}$ dianion. This same study predicts that a N_4^{2-} ring with D_{4h} symmetry should be stable toward geometric distortions and should exhibit 6π aromaticity. Yet another theoretical study[36] which uses a valence-bond correlation diagram model for calculating total distortive energies suggests that, while "free" N_4 and C_4H_4 rings should exhibit significant in-plane rectangular distortion, a square-planar P_4 ring should not possess any such marked tendency to undergo a distortion to a rectangular geometry. Treatment of N_4 and P_4 rings as isolated, noncoordinated systems is of limited relevance to our bonding analysis of **1** in that only metal-coordinated P_4 rings have been characterized and no structures with *cyclo*-N_4 ligands are known.

Fenske–Hall calculations[8] were performed on the hypothetical molecular $W(CO)_4P_4$ fragment of **1**, as well as on the entire molecule, in an attempt to determine the bonding picture of a *cyclo*-P_4 unit coordinated to a metal carbonyl fragment. Figure 5 shows the molecular orbital diagram for $W(CO)_4P_4$, formed from $W(CO)_4$ and P_4 fragments. The filled degenerate HOMOs of this hypothetical $W(CO)_4P_4$ molecule are composed almost entirely of slightly antibonding in-plane P_4 symmetry-adapted combinations of valence 3p P AOs. Thus, while one might expect an oxidized 33-electron monocation to show significant ring distortion, a neutral 34-electron $W(CO)_4$-(η^4-P_4) molecule should not. The doubly degenerate LUMOs (which are 6.1 eV higher in energy than the HOMOs) primarily involve the apical $W(CO)_4$ fragment with large components of bonding $W(5d_\pi)$–$CO(\pi^*)$ orbital character and considerably smaller components of antibonding $W(5d_\pi)$–$P(3p_\pi)$ orbital character.

Molecular orbital calculations for the entire molecule do little to explain the observed distortion of the *cyclo*-P_4

(28) (a) Delbaere, L. T. J.; James, M. N. G.; Nakamura, N.; Masamune, S. *J. Am. Chem. Soc.* **1975**, *97*, 1973. (b) Irngartinger, H.; Rodewald, H. *Angew. Chem., Int. Ed. Engl.* **1974**, *13*, 740. (c) Irngartinger, H.; Riegler, N.; Malsch, K.-D.; Schneider, K.-A.; Maier, G. *Angew. Chem., Int. Ed. Engl.* **1980**, *19*, 211. (d) Irngartinger, H.; Nixdorf, M. *Angew. Chem., Int. Ed. Engl.* **1983**, *22*, 403. (e) Dunitz, J. D.; Krüger, C.; Irngartinger, H.; Maverick, E. F.; Wang, Y.; Nixdorf, M. *Angew. Chem., Int. Ed. Engl.* **1988**, *27*, 387. (f) Irngartinger, H.; Nixdorf, M.; Riegler, N. H.; Krebs, A.; Kimling, H.; Pocklington, J.; Maier, G.; Malsch, K.-D.; Schneider, K.-A. *Chem. Ber.* **1988**, *121*, 673.

(29) X-ray crystallographic determinations[30] of at least 20 cyclobutadiene–metal complexes containing a transition metal coordinated to a cyclobutadiene ligand have shown in the majority of these compounds that the carbon ring has a square-planar geometry within experimental error. However, a comparative examination reveals that deformations of the *cyclo*-C_4R_4 ligand from C_{4v} symmetry and asymmetrical metal-to-C(ring) distances are not uncommon; these geometrical deviations have been attributed to electronic and/or steric effects. To a first approximation, the mean C(ring)–C(ring) distances, which in general are significantly longer that those for metal-coordinated cyclopentadienyl ligands, are not strongly influenced by the ring substituents and/or the nature of the cyclobutadiene–metal complexes. It is noteworthy that a detailed comparison[30d] of the molecular bonding parameters of $Fe(CO)_3(PhC_2C_6H_4C_2Ph)_2Fe(CO)$ with those of $Fe(CO)_3(HOC_2Me)_2Fe(CO)_3$ revealed that the cyclobutadiene ligand may sterically behave as only a bidentate ligand by the effective occupation of two metal coordination sites in place of two terminal carbonyl ligands. Furthermore, the similar orientations of the sterically equivalent Fe(CO)(cyclobutadiene) and $Fe(CO)_3$ fragments relative to the ferracyclopentadiene rings in the respective iron complexes were found to be analogous to the disposition of the Ni(cyclobutadiene) fragment with respect to the ferracyclopentadiene ring in the (Ni–Fe)-bonded $[Fe(CO)_3(MeC_2Me)_2][Ni(C_4Me_4)]$.[30e]

(30) (a) For an excellent general review of cyclobutadiene–metal complexes, see: Efraty, A. *Chem. Rev.* **1977**, *77*, 691 and references therein. (b) Bruce, M. I. Index of Structures Determined by Diffraction Methods. In *Organometallic Chemistry*; Wilkinson, G., Stone, F. G. A., Abel, E. W., Eds.; Pergamon Press: New York, 1982; Vol. 9, pp 1209–1520. (c) Cambridge Structural Database of Organic and Organometallic Compounds, 1989. (d) Epstein, E. F.; Dahl, L. F. *J. Am. Chem. Soc.* **1970**, *92*, 493. (e) Epstein, E. F.; Dahl, L. F. *J. Am. Chem. Soc.* **1970**, *92*, 502.

(31) To our knowledge, there are no examples of a "free" 1,3-diphosphacyclobutadiene ring. Crystallographically characterized metal complexes containing the η^4-coordinated 1,3-diphosphacyclobutadiene ring include $CoCp^*[cyclo\text{-}(PC^tBu)_2]$,[32a] $CoCp[cyclo\text{-}(PC^tBu)_2]$,[32b,c] $Co(\eta^5\text{-indenyl})[cyclo\text{-}(PC^tBu)_2]$,[32c] and $Rh(PMe_3)_2Cl[cyclo\text{-}(PC^tBu)_2]$[32d] (where Cp^* denotes η^5-C_5Me_5, Cp denotes η^5-C_5H_5, η^5-indenyl denotes η^5-C_9H_7, and ^{t}Bu denotes *tert*-butyl). In the above three cobalt complexes, all four P–C bond lengths of each *cyclo*-$(PC^tBu)_2$ ligand are equidistant, and each $(PC)_2$ ring is essentially planar or slightly folded. Consistent with these three cobalt structures, the two P and two C atoms in each $(PC)_2$ ring give rise to only one signal in the ^{31}P and ^{13}C NMR spectra. On the other hand, $Rh(PMe_3)_2Cl[cyclo\text{-}(PC^tBu)_2]$ was found to possess a nonplanar $(PC)_2$ ring with nonequivalent P–C distances and with one Rh–C(ring) distance (trans to the Cl atom) being 0.13 Å shorter than the other Rh–C(ring) distance.[32d] Furthermore, ^{31}P and ^{13}C NMR spectra of this rhodium complex exhibit one and two resonances, respectively, for the $(PC)_2$ ring. In fact, the large difference in the two chemical shifts (δ 84.5, 149.8 ppm) and the spin–spin coupling constants observed in the ^{13}C NMR spectrum led Binger et al.[32d] to propose that the linkage of the $(PC)_2$ ring to the rhodium atom is best described as η^1,η^3 bonding. This proposal is in harmony with Rh(III) coordination to an allyl-like PCP^- monoanion and a C^- monoanion. In this case, the presumed kite-like C_s configuration of the *cyclo*-(1,3-$(PCR)_2$) ring in $Rh(PMe_3)_2Cl[cyclo\text{-}(PC^tBu)_2]$ appears to be electronically induced by the different ligands on the rhodium atom.

(32) (a) Hitchcock, P. B.; Maah, M. J.; Nixon, J. F. *J. Chem. Soc., Chem. Commun.* **1986**, 737. (b) Binger, P.; Milczarek, R.; Mynott, R.; Regitz, M.; Rösch, W. *Angew. Chem., Int. Ed. Engl.* **1986**, *25*, 644. (c) Binger, P.; Milczarek, R.; Mynott, R.; Krüger, C.; Tsay, Y.-H.; Raabe, E.; Regitz, M. *Chem. Ber.* **1988**, *121*, 637. (d) Binger, P.; Biedenbach, B.; Mynott, R.; Krüger, C.; Betz, P.; Regitz, M. *Angew. Chem., Int. Ed. Engl.* **1988**, *27*, 1157.

(33) Hess, B. S.; Ewig, C. S.; Schaad, L. J. *J. Org. Chem.* **1985**, *50*, 5869.

(34) (a) Kettle, S. F. A. *Inorg. Chim. Acta* **1967**, *1*, 303. (b) Elian, M.; Chen, M. M. L.; Mingos, D. M. P.; Hoffmann, R. *Inorg. Chem.* **1976**, *15*, 1148. (c) Mingos, D. M. P. *Adv. Organomet. Chem.* **1977**, *15*, 1.

(35) van Zandwijk, G.; Janssen, R. A. J.; Buck, H. M. *J. Am. Chem. Soc.* **1990**, *112*, 4155.

(36) Ohanessian, G.; Hiberty, P. C.; Lefour, J.-M.; Flament, J.-P.; Shaik, S. S. *Inorg. Chem.* **1988**, *27*, 2219.

ring in 1. Coordination of the Lewis-acid $W(CO)_5$ adducts to $W(CO)_4P_4$ in the molecular species (1) results in two significant changes: (1) the energies of the MOs associated with $W(CO)_4P_4$ are lowered somewhat due to partial orbital mixing with appropriate $W(CO)_5$ orbitals; (2) the W–CO bonding orbitals and tungsten 5d AOs for the four $W(CO)_5$ adducts are the main contributors to the higher energy bonding MOs (including the HOMOs) of 1. Thus, the HOMOs of 1 consist of essentially noninteracting $W(CO)_5$ orbitals. As with the $W(CO)_4P_4$ fragment per se, all orbitals with significant P_4 ring bonding contributions are completely filled, and there is no apparent reason for a P_4 ring distortion to occur. The doubly degenerate LUMOs, which are 4.0 eV higher in energy than the HOMOs, are effectively unchanged in orbital character upon going from $W(CO)_4P_4$ to 1. Although the molecular orbital diagram for 1 does not explain the P_4 ring distortion detected via the ^{31}P NMR data, it is consistent with the lack of reversible electrochemical behavior for 1.

Acknowledgment. This research was generously supported by the National Science Foundation (Grants CHE-8616697 and CHE-9013059). We are most grateful to Dr. Robert Weller (EXTREL FTMS, 8416 Schroeder Rd, Madison, WI 53711) for obtaining LD/FT mass spectra with an EXTREL FTMS-2000 spectrometer. We also thank Ms. Lori Petrovich, Mr. Jackson C. K. Ma, and Ms. Agnes Lee Ma (UW—Madison) for their assistance in obtaining additional ^{31}P and ^{13}C NMR spectra.

Registry No. 1, 136782-25-7; $1\cdot CH_2Cl_2$, 136782-26-8; $W(CO)_6$, 14040-11-0; P_4, 10544-46-4.

Supplementary Material Available: Figures providing the solution and solid-state ^{31}P NMR spectra and tables listing anisotropic displacement coefficients for $W_5(CO)_{24}P_4\cdot CH_2Cl_2$ under *P4nc* symmetry, atomic coordinates, anisotropic displacement coefficients, and selected bond lengths and angles for $W_5(CO)_{24}P_4\cdot CH_2Cl_2$ under *I*4 symmetry, and ion-peak assignments for the LD/FT mass spectra of $W_5(CO)_{24}P_4$ (7 pages); tables of observed and calculated structure factor amplitudes for $W_5(CO)_{24}P_4\cdot CH_2Cl_2$ under *P4nc* and *I*4 symmetry (10 pages). Ordering information is given on any current masthead page.

Synthesis, Stereophysical-Bonding Features, and Chemical–Electrochemical Reactivity of Two Dimetal-Bridging Diphosphide Complexes: $Co_2(\eta^5\text{-}C_5Me_5)_2(\mu_2\text{-}\eta^2\text{-}P_2)_2$ and $Fe_2(\eta^5\text{-}C_5Me_5)_2(\mu_2\text{-}\eta^2\text{-}P_2)_2$

Mary E. Barr[1] and Lawrence F. Dahl*

Department of Chemistry, University of Wisconsin—Madison, Madison, Wisconsin 53706

Received March 5, 1991

Two dimetal-bridging diphosphido complexes, $Co_2Cp^*_2(\mu_2\text{-}\eta^2\text{-}P_2)_2$ (1) and $Fe_2Cp^*_2(\mu_2\text{-}\eta^2\text{-}P_2)_2$ (2) ($Cp^* = \eta^5\text{-}C_5Me_5$), were synthesized by cophotolysis of P_4 with $CoCp^*(CO)_2$ and $Fe_2Cp^*_2(CO)_2(\mu_2\text{-}CO)_2$, respectively. 1 and 2 were characterized from X-ray diffraction, laser-desorption FT mass spectrometric, spectroscopic (^1H, ^{31}P NMR; IR), and electrochemical measurements. An X-ray diffraction study unambiguously showed that the 36-electron cobalt dimer (1) consists of two 14-electron CoCp* fragments linked at a nonbonding Co···Co distance of 3.10 Å by two four-electron-donating η^2-coordinated P_2 ligands. The X-ray crystallographic investigation of the corresponding 34-electron iron dimer (2) disclosed two FeCp* fragments separated by an electron-pair Fe–Fe distance of 2.59 Å; unfortunately, a rotational-type crystal disorder was encountered, which prevented a definitive determination of the number and bonding modes of the bridging phosphorus atoms from the crystallographic analysis per se. However, the X-ray data and a comparative analysis of mass spectral and ^{31}P NMR data for 1 and 2 provide persuasive evidence that the stoichiometry and connectivities of the phosphorus atoms in 2 are identical to those in 1. Cyclic voltammograms indicated that each dimer exhibits reversible oxidative behavior. Preliminary investigations of the potential chemical reactivities of these metal-bridged diphosphide ligands with H_2 and C_2H_4 revealed that they are relatively inert compared to the reactivities previously reported for metal-bridged disulfide ligands with these reagents.

Introduction

As part of our investigations[2] into the photolytic generation of organometallic phosphido complexes, we present herein the photochemical syntheses and characterizations of $Co_2Cp^*_2(\mu_2\text{-}\eta^2\text{-}P_2)_2$ (1) and $Fe_2Cp^*_2(\mu_2\text{-}\eta^2\text{-}P_2)_2$ (2) (where Cp* denotes $\eta^5\text{-}C_5Me_5$). These compounds were prepared from reactions of elemental P_4 with $CoCp^*(CO)_2$ and $[FeCp^*(CO)_2]_2$, respectively. While other organometallic diphosphide complexes are known,[3] 1 and 2 are of particular interest for two reasons. First, the structural elucidation of the mode of coordination of the four bridging phosphorus atoms in the (pentamethylcyclopentadienyl)cobalt dimer (1) as two η^2-P_2 ligands clarifies the previously reported ambiguous crystallographic evidence that its (tetramethylethylcyclopentadienyl)cobalt analogue may contain a *cyclo*-P_4 ligand.[3b,4] Second, isolation of 1 and 2 in our laboratory afforded the opportunity to instigate preliminary investigations into the chemical reactivity of metal-bridged diphosphide ligands toward

(1) Present address: Los Alamos National Laboratory, University of California, Los Alamos, NM 87545.

(2) (a) Barr, M. E.; Adams, B. R.; Weller, R. R.; Dahl, L. F.; *J. Am. Chem. Soc.* **1991**, *113*, 3052. (b) Barr, M. E.; Smith, S. K.; Spencer, B.; Dahl, L. F. *Organometallics*, preceding paper in this issue.

(3) (a) DiViara, M.; Stoppioni, P.; Peruzzini, M. *Polyhedron* **1987**, *6*, 351 and references therein. (b) Scherer, O. J. *Comments Inorg. Chem.* **1987**, *6*, 1. (c) Scherer, O. J. *Angew. Chem., Int. Ed. Engl.* **1985**, *24*, 924.

(4) Scherer, O. J.; Swarowsky, M.; Wolmershäuser, G. *Angew. Chem., Int. Ed. Engl.* **1988**, *27*, 405.

0276-7333/91/2310-3991$02.50/0